New Detailed Understanding of the Mechanism of Radiation in Interconnect Problems

Ying S. Cao[#1], Li Jun Jiang[#2], Albert E. Ruehli[+3], Jun Fan[+4], and James. L. Drewniak[+5]
[#] *The University of Hong Kong, Pokfulam Road, Hong Kong*
[1] *caoying@eee.hku.hk,* [2] *jianglj@hku.hk*
[+] *EMC Laboratory, Missouri University of Science and Technology, Rolla, MO, 65401, USA*
[3] *albert.ruehli@gmail.com,* [4] *jfan@mst.edu,* [5] *drewniak@mst.edu*

***Abstract*—Electromagnetic radiations from parasitic structures such as electronic interconnections are very difficult to diagnose because the ability to identify the specific sources are missing. Mainly, the source of radiations cannot be identified separately. Here, the partial element equivalent circuit (PEEC) method is extended to diagnose the radiation and its distribution. For the first time we identify the individual sources of radiation and the equivalence circuits for the sources. The proposed approach can be applied to find the radiation for electromagnetic interference (EMI) from a wide variety of structures.**

I. Introduction

The prediction of radiated power for parasitic structures such as interconnects is of great interest because excessive radiation can impact the functioning of electronic equipment or it may cause interference problems. For this reason, the analysis of the radiated power has been considered by many researchers, e.g., [1]–[3].

High-speed connectors are used as part of the signal transmission path between multilayer printed circuit boards (PCB). In order to model more details, the separate radiation of all different parts of a structure was developed [4]. Connectors can be major sources for radiation of systems in the gigahertz range [5], [6]. Two basic kinds of connectors are used, backplane connectors and optical cage connectors.

Recently, a more detailed investigation of the sources of radiation was presented in [7]. The details of the Partial Element Equivalent Circuit (PEEC) solution leads to additional important new insights into the radiation mechanism. The PEEC method is used to establish a connection between retardation and the partial elements, which we show is of fundamental importance.

Today, the PEEC method is a well-known integral equation based approach [8]. Electric field integral equation (EFIE) with potentials and currents as unknowns leads to comprehensive models. The approach turns the electromagnetic fields into a circuit problem where the capacitive and inductive behaviors can be studied in detail. Information about each fundament loop in the equivalent circuit is available. In this approach, all local power dissipation results at a loop-by-loop can be found. Here we show, how the coupling between the partial elements leads to the determination of radiation.

The paper is organized as follows: Section II gives a brief introduction to the PEEC formulations for calculating both the total radiation and radiation from parts of the geometry; Section III discusses the physical interpretation of radiation mechanism and Section IV gives numerical examples to support the theoretical aspects.

II. PEEC circuit formulation

For this short paper we keep the details of the PEEC method very brief. The usual EFIE electric field at a conductors given by

$$\mathbf{E}_0(\mathbf{r},t) = \frac{\mathbf{J}(\mathbf{r},t)}{\sigma} + \frac{\partial \mathbf{A}(\mathbf{r},t)}{\partial t} + \nabla\Phi(\mathbf{r},t) \qquad (1)$$

where $\mathbf{E}_0$ is a potential applied electric field, $\mathbf{J}$ is the current density in the conductors, $\mathbf{A}$ and Φ are vector and scalar potentials, respectively. The general full-wave volume (Lp,P,R,τ) PEEC model with delays τ based on (1) includes voltage sources corresponding to the left hand side and resistances, partial inductances and capacitances corresponding to the right hand side terms [8].

As described in detail in [9], the left-hand side of (1) represents potential external fields which we assume to be zero for this work. In PEEC, the first term on the right hand side can be transformed into resistors, the second term into partial inductances and the last term into capacitive models represented by partial coefficients of potential. Each fundamental loop of the PEEC equivalent circuit is as shown in Fig. 1. The resultant MNA circuit equations [10] for multiple

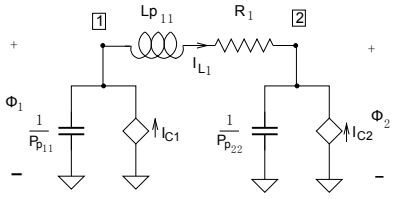

Fig. 1. Example of a single PEEC equivalent circuit loop.

loops as given in the equivalent circuit (1) are

$$\begin{bmatrix} s\mathbf{P}p^{-1} & \mathbf{A} \\ \mathbf{A}^T & -(\mathbf{R}+s\mathbf{L}p) \end{bmatrix} \cdot \begin{bmatrix} \mathbf{\Phi} \\ \mathbf{I} \end{bmatrix} = \begin{bmatrix} \mathbf{I}_i \\ \mathbf{V}_i \end{bmatrix}. \qquad (2)$$

III. Retardation with the Radiation

For simplicity, we assume that the radiating structure does not include loss models such as skin-effect or dielectric losses.

Hence, in Fig. 1 the loss resistors like R_1 are set to zero. If we apply Poynting's theorem in integral form [11]:

$$-\frac{1}{2}\int_S (\mathbf{E}\times\mathbf{H}^*)\cdot\hat{\mathbf{n}}dS = \frac{1}{2}j\omega\int_V \left(\mu_0|\mathbf{H}|^2-\varepsilon|\mathbf{E}|^2\right)dV + \frac{1}{2}\int_V \mathbf{E}\cdot\mathbf{J}^*\,dV. \quad (3)$$

The integral on the left represents the total power leaving a surface. For the far field, this surface is moved far enough from the structure under investigation. Then, only the contributions which decay with $1/R$ are taken into account, while the local fields for the circuit elements are not contributing. The far-field model reduces the time average radiation through the surface to

$$-\frac{1}{2}\mathrm{Re}\int_S (\mathbf{E}\times\mathbf{H}^*)\cdot\hat{\mathbf{n}}dS = \frac{1}{2}\mathrm{Re}\int_V \mathbf{E}\cdot\mathbf{J}^*\,dV. \quad (4)$$

From the PEEC equivalent circuit in Fig. 1, we can see that if the resistive loss is not considered, then there are only the energy storage elements. It seems to be contradictory to (4) since only the real part of the integral is contributing to the far field radiation. In the next section, we consider this issue.

Through analysis, this contradiction hints at the relationship between the retardation and the radiation. Specifically, the partial inductance with retardation in the frequency domain is given by

$$Lp_{12}^R = \frac{\mu_0}{4\pi}\frac{1}{A_1A_2}\int_{V_1}\int_{V_2}\frac{e^{-jkR_{12}}}{R_{12}}\,dV_2\,dV_1 \quad (5)$$

where $R_{12}=|\mathbf{r}_1-\mathbf{r}_2|$, the cell size for each of the conductor volumes is limited to be equal or smaller than $\lambda_{min}/20$ in the largest length. To illustrate the issue at hand we expand the exponential function as $exp(-jkR_{12}) = cos(kR_{12}) - jsin(kR_{12})$. Since the cell sizes are relatively small, we can approximate the inductive impedance of (5) as

$$Z_L = j\omega Lp_{12}^R \approx j\omega cos(kR_{12})Lp_{12} + \omega sin(kR_{12})Lp_{12} \quad (6)$$

to gain some key insight. Similarly, we can rewrite the partial coefficients of potential to include the retardation using the above approximation.

$$Pp_{12}^R = \frac{1}{4\pi\varepsilon_0}\frac{1}{S_1S_2}\int_{S_1}\int_{S_2}\frac{e^{-jkR_{12}}}{R_{12}}\,dS_2\,dS_1 \quad (7)$$

We use the same approximation of the exponential term to study the impact of the retardation on a single term to find

$$Z_C = -j\frac{cos(kR_{12})Pp_{12}}{\omega} - \frac{sin(kR_{12})Pp_{12}}{\omega}. \quad (8)$$

The negative capacitive impedance for lower frequencies reminds us of the capacitance in a resonance circuit. Further interesting conclusions can be made:

Observation 1: From (4) it is evident that only the real part of the circuit can contribute to the radiated power. It is clear from this formulation and the equivalent circuit that the source of far field radiation can only be due to the inductive and capacitive retardation.

These observations are better formulated by (6) and (8). The inductive contribution to the radiation at low frequencies and close couplings is that positive contributions are made to the radiation resistance and equally, to the radiated power. Larger distance results in larger retardation. With the given frequency, the retardation will control the radiation efficiency through the sin function. It means that on top of the $1/R^2$ attenuation, the distributive parts have repeated peaks and valleys for the radiation enhancements.

Another important observation is due at this point. The positive real parts of the radiation dominates over the negative parts since the interconnect or antenna structure is clearly passive. The detailed PEEC equivalent circuit for a structure consists of a multitude of $L-C$ resonance circuits which for each applied frequency f.

Observation 2: We understand that the retarded coupling has a positive or negative reactance contribution depending on the frequency f and the distance R between the coupled cells. This leads to a multitude of potentially positive and negative local contributions to the radiated power.

These observations lead to the fundamental insight into the contributions of the different parts of a radiation structure to the total radiated power. As we show in the next section, we have the ability to compute the power for each partial element or part of a structure of the geometry. Hence, we can in detail analyze a radiating structure.

IV. Numerical Examples

A. Model for two coupled PEEC loops

A two-loop model by PEEC is illustrated in Fig. 2. We assume that the two loops which are part of a complex model are spaced at a distance s

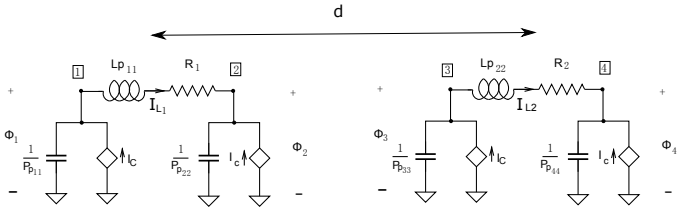

Fig. 2. A two-cell model by PEEC.

If the working frequency is to be 75 MHz, and the two cells are 1/20 wavelengths long. The distance d is set to be zero. The retardation terms in the inductive and capacitive branches lead to the radiation loss.

The capacitive contributions are listed in detail as

$$\begin{pmatrix} P_C^{11r} & P_C^{12r} & P_C^{13r} & P_C^{14r} \\ P_C^{21r} & P_C^{22r} & P_C^{23r} & P_C^{24r} \\ P_C^{31r} & P_C^{32r} & P_C^{33r} & P_C^{34r} \\ P_C^{41r} & P_C^{42r} & P_C^{43r} & P_C^{44r} \end{pmatrix} =$$

$$\frac{1}{2}\mathrm{Re}\frac{1}{s}\begin{pmatrix} I_1^{C*}Pp_{11}I_1^C & I_1^{C*}Pp_{12}I_2^C & I_1^{C*}Pp_{13}I_3^C & I_1^{C*}Pp_{14}I_4^C \\ I_2^{C*}Pp_{21}I_1^C & I_2^{C*}Pp_{22}I_2^C & I_2^{C*}Pp_{23}I_3^C & I_2^{C*}Pp_{24}I_4^C \\ I_3^{C*}Pp_{31}I_1^C & I_3^{C*}Pp_{32}I_2^C & I_3^{C*}Pp_{33}I_3^C & I_3^{C*}Pp_{34}I_4^C \\ I_4^{C*}Pp_{41}I_1^C & I_4^{C*}Pp_{42}I_2^C & I_4^{C*}Pp_{43}I_3^C & I_4^{C*}Pp_{44}I_4^C \end{pmatrix}. \quad (9)$$

Also,

$$P_C^{mr} = \sum_{n=1}^{4} P_C^{mnr}, \quad m = 1, 2, 3 \text{ and } 4. \tag{10a}$$

$$P_C^{r} = \sum_{m=1}^{4} P_C^{mr}. \tag{10b}$$

P_C^{mr} is the radiated power in the m-th capacitive branch, and P_C^r is the radiated power for the total capacitive branches.

The definition of the coefficient of potential Pp is defined as

$$Pp_{mn} = \frac{1}{\varepsilon S_m S_n} \int_{S_m} \int_{S_n} \frac{e^{-jk|\mathbf{r}_m - \mathbf{r}_n|}}{|\mathbf{r}_m - \mathbf{r}_n|} dS_m dS_n. \tag{11}$$

Therefore,

$$\begin{aligned} P_C^{mnr} &\propto \mathrm{Re}\{\frac{1}{s} I_m^{C*} \frac{e^{-jk|\mathbf{r}_i - \mathbf{r}_j|}}{|\mathbf{r}_i - \mathbf{r}_j|} I_n^C\} \\ &\propto \mathrm{Re}\{I_m^{C*} \frac{\frac{1}{s}\cos(k\,|\mathbf{r}_i - \mathbf{r}_j|) - \frac{1}{\omega}\sin(k\,|\mathbf{r}_i - \mathbf{r}_j|)}{|\mathbf{r}_i - \mathbf{r}_j|} I_n^C\} \end{aligned} \tag{12}$$

at low frequency range, $k\,|\mathbf{r}_i - \mathbf{r}_j| < \pi/2$. For this, the real part of Pp_{mn}/s stays negative.

The currents in the capacitive branches shown in Fig. 2 are

$$I_1^C = -8.64 \times 10^{-5} j \tag{13a}$$

$$I_2^C = -9.20 \times 10^{-5} j \tag{13b}$$

$$I_3^C = 9.20 \times 10^{-5} j \tag{13c}$$

$$I_4^C = 8.64 \times 10^{-5} j \tag{13d}$$

By combining (9), (11), (12) and (13), the sign of all the P_C^{mnr} can be determined as

$$\begin{pmatrix} P_C^{11r} & P_C^{12r} & P_C^{13r} & P_C^{14r} \\ P_C^{21r} & P_C^{22r} & P_C^{23r} & P_C^{24r} \\ P_C^{31r} & P_C^{32r} & P_C^{33r} & P_C^{34r} \\ P_C^{41r} & P_C^{42r} & P_C^{43r} & P_C^{44r} \end{pmatrix} \Rightarrow \begin{pmatrix} - & - & + & + \\ - & - & + & + \\ + & + & - & - \\ + & + & - & - \end{pmatrix}. \tag{14}$$

where we use '+' and '-' to mean that the corresponding radiated power is either positive or negative. The interesting local power results have different signs and different absolute values which are comparable with each other.

The analysis for the partial inductances for neighboring cells is more intuitive. At very low frequency, I_{L1} and I_{L2} are almost the same and the real part of sLp_{ij} is positive. For this case, the sign for the P_L^{ijr} can be determined as

$$\begin{pmatrix} P_L^{11r} & P_L^{12r} \\ P_L^{21r} & P_L^{22r} \end{pmatrix} \Rightarrow \begin{pmatrix} + & + \\ + & + \end{pmatrix}. \tag{15}$$

Based on (14) and (15), the radiated power for each local loop is the combination of the inductive and the capacitive power.

$$\begin{aligned} P_1^r =& P_L^{1r} + P_C^{1r} + P_C^{2r} \\ =& P_L^{11r} + P_L^{12r} + P_C^{11r} + P_C^{12r} + P_C^{13r} + P_C^{14r} \\ &+ P_C^{21r} + P_C^{22r} + P_C^{23r} + P_C^{24r} \\ \Rightarrow& (+) + (+) + (-) + (-) + (+) + (+) \\ &+ (-) + (-) + (+) + (+) \end{aligned} \tag{16}$$

In general, it is obvious from (5) and (8) that for distant cells, both the partial inductances and the partial potential coefficients as well as the retarded parts can be positive or negative leading to very interesting results. We notice that in the frequency domain, the key parameters for the sign of the elements depends strongly on the distance d and the frequency f.

V. Conclusion

The radiation from each cell in a geometrical model can be evaluated in the PEEC based approach presented in this paper. This formulation allows to gain new details insights into the behavior of radiating structures. We show that we can predict parts of a structure which contribute more or less radiation. The next step is clearly that guidelines are derived based on this work for radiating structures like connectors and other parts for mitigating radiation.

References

[1] L. K. Yeung and K.-L. Wu, "Generalized partial element equivalent circuit (PEEC) modeling with radiation effect," *IEEE Transactions on Microwave Theory and Techniques*, vol. 59, no. 10, pp. 2377–3384, Oct. 2011.

[2] M. Valek, M. Leone, and F. Schmiedl, "Analysis of the electromagnetic radiation behavior of motherboard-subboard structures," in *Proc. of the IEEE Int. Symp. on Electromagnetic Compatibility*, Chicago, USA, Aug. 2005, pp. 175–178.

[3] J. Nitsch, F. Gronnwald, and G. Wollenberg, *Radiating nonuniform transmission-line systems and the partial element equivalent circuit method*. John Wiley and Sons, New York, 2009.

[4] Y. S. Cao, L. J. Jiang, and A. E. Ruehli, "Distributive radiation and transfer characterization based on the PEEC method," *IEEE Transactions on Electromagnetic Compatibility*, vol. 57, Aug. 2015.

[5] X. Tian, M. S. Halligan, L. Gui, X. Li, K. Kim, S. Connor, B. Archambeault, M. Cracraft, A. Ruehli, Q. Li, D. Pommerenke, and J. L. Drewniak, "Quantifying radiation and physics form edge-coupled signal connectors," *IEEE Transactions on Electromagnetic Compatibility*, vol. 57, Aug. 2015.

[6] A. Vukicevic, F. Rachidi, M. Rubinstein, and S. V. Tkachenko, "On the evaluation of antenna-mode currents along transmission lines," *IEEE Transactions on Electromagnetic Compatibility*, vol. 48, no. 4, pp. 693–700, Nov. 2006.

[7] Y. S. Cao, L. J. Jiang, and A. E. Ruehli, "Physical interpretation of radiation and transfer characterization based on the PEEC method," in *Proc. of the IEEE Int. Symp. on Electromagnetic Compatibility*, Aug. 2015.

[8] A. E. Ruehli, G. Antonini, J. Esch, J. Ekman, A. Mayo, and A. Orlandi, "Non-orthogonal PEEC formulation for time and frequency domain EM and circuit modeling," in *Proc. of the IEEE Int. Symp. on Electromagnetic Compatibility*, vol. 45, May 2003, pp. 167–176.

[9] A. E. Ruehli, G. Antonini, and L. Jiang, *The partial element equivalent circuit method for electromagnetic and circuit problems*. John Wiley and Sons, New York, 2016.

[10] C. Ho, A. E. Ruehli, and P. Brennan, "Interactive circuit analysis and design using APL," in *Proc. of the IEEE Int. Symp. on Circuits and Systems*, May 1975.

[11] J. A. Kong, *Electromagnetic Wave Theory*. Cambridge, Massachusetts, USA: EMW Publishing, 2008.